THE JOURNAL OF BIOLOGICAL CHEMISTRY VOL. 288, NO. 7, pp. 5166–5175, February 15, 2013

Functional Separation of Endosomal Fusion Factors and the Class C Core Vacuole/Endosome Tethering (CORVET) Complex in Endosome Biogenesis*[S]

Received for publication, October 29, 2012, and in revised form, December 12, 2012 Published, JBC Papers in Press, December 22, 2012, DOI 10.1074/jbc.M112.431536

Margarita Cabrera[‡1], Henning Arlt[‡], Nadine Epp[‡], Jens Lachmann[‡], Janice Griffith[§], Angela Perz[‡], Fulvio Reggiori[§], and Christian Ungermann[‡2]

From the [‡]University of Osnabrück, Department of Biology/Chemistry, Biochemistry Section, Barbarastr. 13, 49076 Osnabrück, Germany and the [§]University Medical Centre Utrecht, Department of Cell Biology and Institute of Biomembranes, Heidelberglaan 100, 3584 CX Utrecht, The Netherlands

Background: The interdependence of the endosomal fusion factors CORVET and Vac1 has not been addressed.
Results: CORVET can be separated from other endocytic fusion factors on the basis of ultrastructure, localization, and trafficking.
Conclusion: CORVET acts independently of the Vac1 tether and requires activated Rab5 homologs for localization.
Significance: Our data reveal a unique role of CORVET in sorting of biosynthetic cargo to the vacuole.

Transport along the endolysosomal system requires multiple fusion events at early and late endosomes. Deletion of several endosomal fusion factors, including the Vac1 tether and the Class C core vacuole/endosome tethering (CORVET) complex-specific subunits Vps3 and Vps8, results in a class D *vps* phenotype. As these mutants have an apparently similar defect in endosomal transport, we asked whether CORVET and Vac1 could still act in distinct tethering reactions. Our data reveal that CORVET mutants can be rescued by Vac1 overexpression in the endocytic pathway but not in CPY or Cps1 sorting to the vacuole. Moreover, when we compared the ultrastructure, CORVET mutants were most similar to deletions of the Rab Vps21 and its guanine nucleotide exchange factor Vps9 and different from *vac1* deletion, indicating separate functions. Likewise, CORVET still localized to endosomes even in the absence of Vac1, whereas Vac1 localization became diffuse in CORVET mutants. Importantly, CORVET localization requires the Rab5 homologs Vps21 and Ypt52, whereas Vac1 localization is strictly Vps21-dependent. In this context, we also uncover that Muk1 can compensate for loss of Vps9 in CORVET localization, indicating that two Rab5 guanine nucleotide exchange factors operate in the endocytic pathway. Overall, our study reveals a unique role of CORVET in the sorting of biosynthetic cargo to the vacuole/lysosome.

The endolysosomal system consists of strongly interconnected organelles. Endosomes form and mature as a result of constant fusion events. They receive their membrane and protein load via endocytosis from the plasma membrane and from Golgi-derived vesicles that deliver, among others, vacuolar hydrolases. Within the yeast endocytic pathway, we distinguish early endosomes and late endosomes (also called prevacuolar compartment or multivesicular body) (1–4). Many lines of evidence suggest that early endosomes mature into late endosomes, which is accompanied by recycling of cargo receptors back to the Golgi and plasma membrane mediated by the retromer and Snx4/41/42 complexes (5–7). In addition, ubiquitinated membrane proteins are sorted into intraluminal vesicles of late endosomes by the endosomal sorting complex required for transport (ESCRT) machinery (8–13). Maturation of early to late endosomes also requires a change of the fusion machinery components on the organelle and includes loss of Rab5/Vps21 and gain of Rab7/Ypt7 before the mature late endosome can fuse with the vacuole (1, 3, 14–16).

In general, fusion between membranes requires a lipid bilayer-bound Rab GTPase such as the mentioned Rab5 and Rab7 proteins, which interacts in its active GTP form with a tethering complex or protein to bring membranes into close contact. Subsequently, membrane-anchored SNAREs (soluble *N*-ethylmaleimide-sensitive factor attachment protein receptor) on both membranes form four-helix bundles and trigger bilayer mixing. Within the secretory pathway, CATCHR (complexes associated with tethering containing helical rods) complexes like the exocyst at the plasma membrane and the COG (conserved oligomeric Golgi) complex at the Golgi have been identified, whereas the Vps class C complexes, namely the CORVET and the HOPS (homotypic fusion and vacuole protein sorting) complexes, are necessary within the endolysosomal system (5, 7, 16–18). CORVET and HOPS are both heterohexamer complexes that share the Vps11, Vps16, Vps18, and Vps33 subunits (8, 10, 12). Because of their inclusion in two tethering complexes, their deletions result in a massive fragmentation of the

* This work was supported by Sonderforschungsbereich (SFB) 944 (project P11); by the Hans Mühlenhoff Foundation (to C. U.); and by European Community Humanitarian Office (ECHO) Grant 700.59.003, Earth and Life Science ALW Open Program Grant 821.02.017, and Deutsche Forschungsgemeinschaft-Netherlands Organisation for Scientific Research (DFG-NWO) Cooperation Grant DN 82-303 (to F. R.) and UN111/7-1 (to C. U.).
[S] This article contains supplemental Tables S1 and S2.
[1] To whom correspondence may be addressed: Department of Biology/Chemistry, Biochemistry Section, Barbarastr. 13, 49076 Osnabrück, Germany. Fax: 49-541-969-2884 or -3422; E-mail: Margarita.Cabrera@biologie.uni-osnabrueck.de.
[2] To whom correspondence may be addressed: Department of Biology/Chemistry, Biochemistry Section, Barbarastr. 13, 49076 Osnabrück, Germany. Fax: 49-541-969-2884 or -3422; E-mail: cu@uos.de.

vacuole, which has been termed class C phenotype (Fig. 1*A*) (2). CORVET has two Rab-specific subunits, Vps3 and Vps8, which both interact with Vps21-GTP (14–16). The homologous Vps39 and Vps41 counterparts within HOPS bind to Ypt7-GTP (16–18). Recent structural data show that HOPS forms an elongated particle where the Rab-interacting subunits localize to opposite ends, which can explain its ability to drive tethering of Ypt7-containing membranes (18). HOPS and CORVET share the Sec1/Munc18-like Vps33 subunit, which is the interaction site for SNARE complexes (19–21).

On the basis of its homology to HOPS, the CORVET complex has been postulated to act as a tethering complex as well (2, 4, 12, 14). However, it has remained challenging to find solid evidence supporting such a function. In addition, data on the precise interplay of CORVET with other endosomal fusion factors are lacking. Endosome biogenesis requires several proteins implicated in fusion, including the guanine nucleotide exchange factor (GEF)[3] Vps9, which activates Vps21 (6, 22). The Rab5 homolog Vps21 can in turn bind the EEA1-like Vac1 tether, which also contains a binding site for phosphoinositide-3-phosphate (23, 24). This tethering machinery interacts with the SNARE Pep12 and its Sec1/Munc18 protein Vps45 to fuse transport vesicles at the endosomes (9, 11, 13, 24). Additional fusion events at the early and late endosome may require the CORVET complex (12, 14) (Fig. 1*A*). Importantly, deletions of the CORVET subunits Vps3 and Vps8 result in a similar phenotype like deletions of *VPS9*, *VPS21*, *VPS45*, *VAC1*, or *PEP12*, which have been classified as class D genes (1, 3, 25–27). The vacuoles of the class D mutants are larger than wild-type vacuoles, do not fragment upon salt stress, and thus have deficiencies in vacuole inheritance (28). For cells lacking Vps8, we showed previously that the resulting vacuoles contain both Vps21 and Ypt7, indicating a defect in endosomal maturation (12).

In this study, we set out to reveal the interplay of CORVET with other endosomal fusion factors of the same morphological class. In particular, we compared Vps3 and Vps8 with Vac1, as all proteins operate in tethering events. Several lines of evidence, including a detailed ultrastructural analysis of all class D mutants, support the idea that CORVET acts independently of Vac1 in the biosynthetic and endocytic pathways. We show that two Rab5 proteins, Vps21 and Ypt52, confer CORVET localization to endosomes. Moreover, this localization depends on two redundant GEFs, the previously characterized Vps9 and Muk1, a predicted Vps9 GEF (29). The same Vps9 domain is also found in several mammalian Rab5 GEFs (29). Our data provide further *in vivo* support for CORVET function as an endosome-specific tethering factor.

EXPERIMENTAL PROCEDURES

Yeast Strains and Molecular Biology—All yeast strains and plasmids used in this study are listed in supplemental Tables S1 and S2, respectively. Tagging of proteins was performed by homologous recombination of the tag and the marker at the 5′ or 3′ end of the gene (30). Alternatively, plasmids encoding for tagged constructs were integrated into the genome. In brief, dsRed-tagged Vps21 and Pep12 were expressed from pRS-based vectors under the control of the *PHO5* promoter. The Vps3-GFP and Vps8-GFP constructs were expressed from pRS415-*NOP1*pr plasmids. GFP-tagged alleles were amplified from genomic DNA and subcloned into the pRS415-*NOP1*pr plasmid using NotI and XhoI. The *NOP1* promoter was used for expression levels comparable with WT. Expression of Muk1 and Vps9 fused to the MBP was performed in BL21 Rosetta. Protein production was induced with 0.5 mM isopropyl 1-thio-β-D-galactopyranoside for 16 h at 16 °C. Cells were lysed in buffer containing 20 mM Tris-HCl (pH 7.4), 200 mM NaCl, 1 mM EDTA, 1 mM DTT, 1 mM PMSF, and protease inhibitor mixture (Roche). Proteins were purified using amylose resin (New England Biolabs, Inc., Ipswich, MA) and eluted by addition of 10 mM maltose. GST-tagged Rabs were expressed in BL21 Rosetta upon addition of 0.5 mM isopropyl 1-thio-β-D-galactopyranoside. After growth for 16 h at 16 °C, cells were lysed in PBS containing 1 mM PMSF and protease inhibitor mixture (Roche). Proteins were purified using GSH beads (GE Healthcare) and eluted with 20 mM glutathione. Buffer exchange was performed using PD10 column (GE Healthcare).

Microscopy—Yeast cells were grown to mid-log phase in yeast peptone dextrose (YPD), yeast peptone galactose (YPG), or synthetic dextrose complete (SDC) medium lacking selected amino acids or nucleotides, collected by centrifugation, washed once with SDC medium supplemented with all amino acids, and immediately analyzed by fluorescence microscopy. For FM4-64 staining of vacuoles, cells were incubated with 30 μM FM4-64 for 30 min, washed twice with YPD medium, and incubated in the same medium without dye for 1 h. Images were acquired with a Leica DM5500 B microscope equipped with a SPOT Pursuit camera equipped with an internal filter wheel (D460sp, BP460-515 and D580lp, Leica Microsystems GmbH, Germany), fluorescence filters (49002 ET-GFP (FITC/Cy2): excitation ET470/×40, emission ET525/50 m; wide green: excitation D535/50, emission E590lp; 49008 ET-mCherry, Texas Red: excitation ET560/×40, emission ET630/75 m; Chroma Technology Corp.), and Metamorph 7 software (Visitron Systems, Munich, Germany). Images were processed using ImageJ 1.42 (National Institutes of Health).

Electron microscopy of Epon-embedded cells was done as described previously (14, 31, 32). Statistical evaluation of the EM sections was performed by 50 randomly selected cell profiles and counting of the number of vesicles and putative endosomal structures. Vesicles were defined as circular or tubular structures with a diameter up to 80 nm, whereas putative endosomes were considered to be large circular structures with a dark content and/or stacks of membranes.

Canavanine Assay—Cells were grown in YPD to logarithmic phase, diluted to A_{600} = 0.25, and serial dilutions (1:5) were spotted onto SDC plates without arginine containing the indicated canavanine concentrations. Plates were imaged after 4 days of growth at 30 °C.

Invertase Assay—Yeast strain BHY10 (33) containing *VAC1* expression plasmids was grown in synthetic medium to logarithmic phase and spotted onto synthetic medium containing

[3] The abbreviations used are: GEF, guanine nucleotide exchange factor; MBP, maltose binding protein; SDC, synthetic dextrose complete; CPY, carboxypeptidase Y.

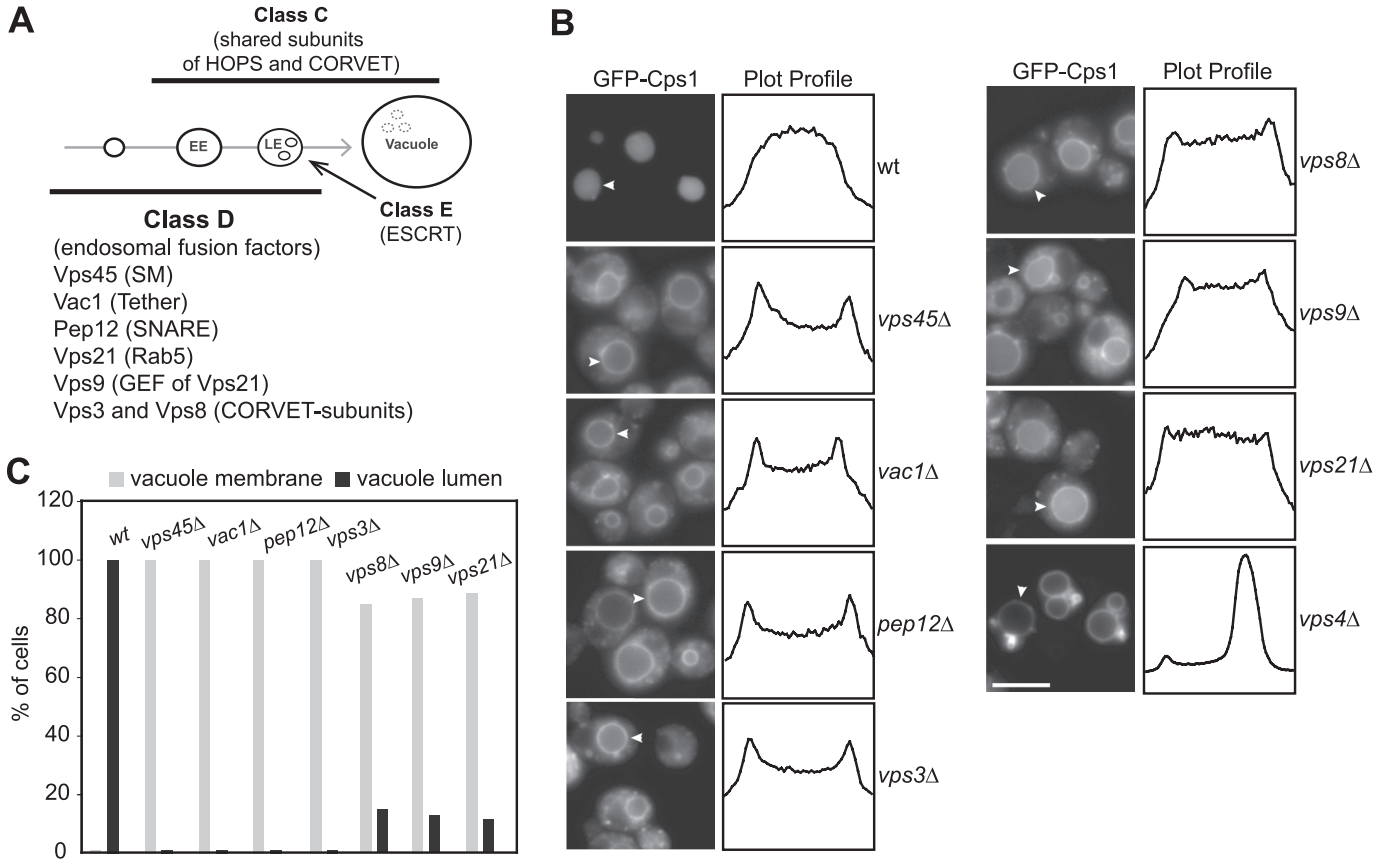

FIGURE 1. **Sorting of Golgi-derived cargo in class D mutants.** *A*, overview of proteins that operate in membrane remodeling and fusion at the endosome and vacuole. Classes refer to the previously identified morphological groups (1). *EE*, early endosome; *LE*, late endosome; *ESCRT*, endosomal sorting complex required for transport; *SM*, Sec1/Munc18. *B*, Cps1 sorting defect in class D mutants. Cps1 was genomically tagged at its N terminus with GFP in WT and the indicated deletion strains. Cells were then analyzed by fluorescence microscopy. Fluorescence intensity profiles of representative vacuoles (*white arrowheads*) are shown. *Scale bar* = 5 μm. See "Experimental Procedures" for details. *C*, quantitative analysis of Cps1 distribution in class D mutants ($n > 100$).

2% fructose as described for the canavanine assay. After 3 days of growth at 30 °C, CPY invertase secretion was analyzed by overlaying plates with developer solution (33).

Fluorescent GEF Assay—GEF assays were performed as described in Ref. 34. Briefly, 500 pmol of GST-Rabs preloaded with 2/3 O-(*N*-methylanthraniloyl) (MANT)-GDP were incubated with different amounts of MBP-Vps9 or MBP-Muk1. After 200 s, 0.1 mM GTP was added to trigger the exchange reaction. MANT fluorescence was monitored using a fluorimeter with a temperature-controlled cuvette and a stirring device (Jasco, Gross-Umstadt, Germany). Excitation was performed at 366 nm, and emission was measured at 443 nm.

RESULTS

Class D Mutants Differ in their Endosomal Transport Defects—The biogenesis of the yeast vacuole (lysosome) is closely linked to trafficking toward the early and late endosomes. Consequently, any perturbation in the fusion machinery at the early and late endosome will cause vacuolar protein transport defects and results in a similar phenotype, the enlarged class D vacuole (2, 25–27). Seven class D mutants have been identified over the last years. Previous data provided support that five factors, the Rab5 GTPase Vps21, its GEF Vps9, the Q-SNARE Pep12, the Sec1/Munc18-like Vps45 protein, and EEA1-like Vac1 protein cooperate at the early endosome (23, 24). With the identification of the CORVET complex, it was assumed that CORVET acts independently of the Vac1-mediated tethering at early endosomes (12, 14), although the possible interdependence was not addressed in any previous study. We decided to address this issue by comparing the different mutants and following the localization of both tethers.

We first asked whether loss of the class D mutants had similar effects on the delivery of biosynthetic cargo to the vacuole and, therefore, followed the sorting of the GFP-tagged Golgi-derived cargo Cps1. In wild-type cells, Cps1 is sorted at late endosomes into intraluminal vesicles with the help of the ESCRT complexes and subsequently accumulates in the vacuole lumen (Fig. 1*B*). In ESCRT mutants like *vps4*Δ, sorting into the intraluminal vesicles is impaired, and GFP-Cps1 is found on the limiting membrane of the vacuole and aberrant endosomes (35) (Fig. 1*B*). In all class D mutants, we observed that Cps1 also accumulated on the vacuole rim and in vesicular structures, indicating that the loss of efficient endosomal fusion strongly affects cargo delivery to the vacuole (Fig. 1, *B* and *C*). In contrast, cargo sorting via the AP-3 pathway, which bypasses the endosomal compartment, was functional in all class D mutants (not shown).

Next, we asked whether transport from the plasma membrane to the vacuole is equally defective in all mutants and,

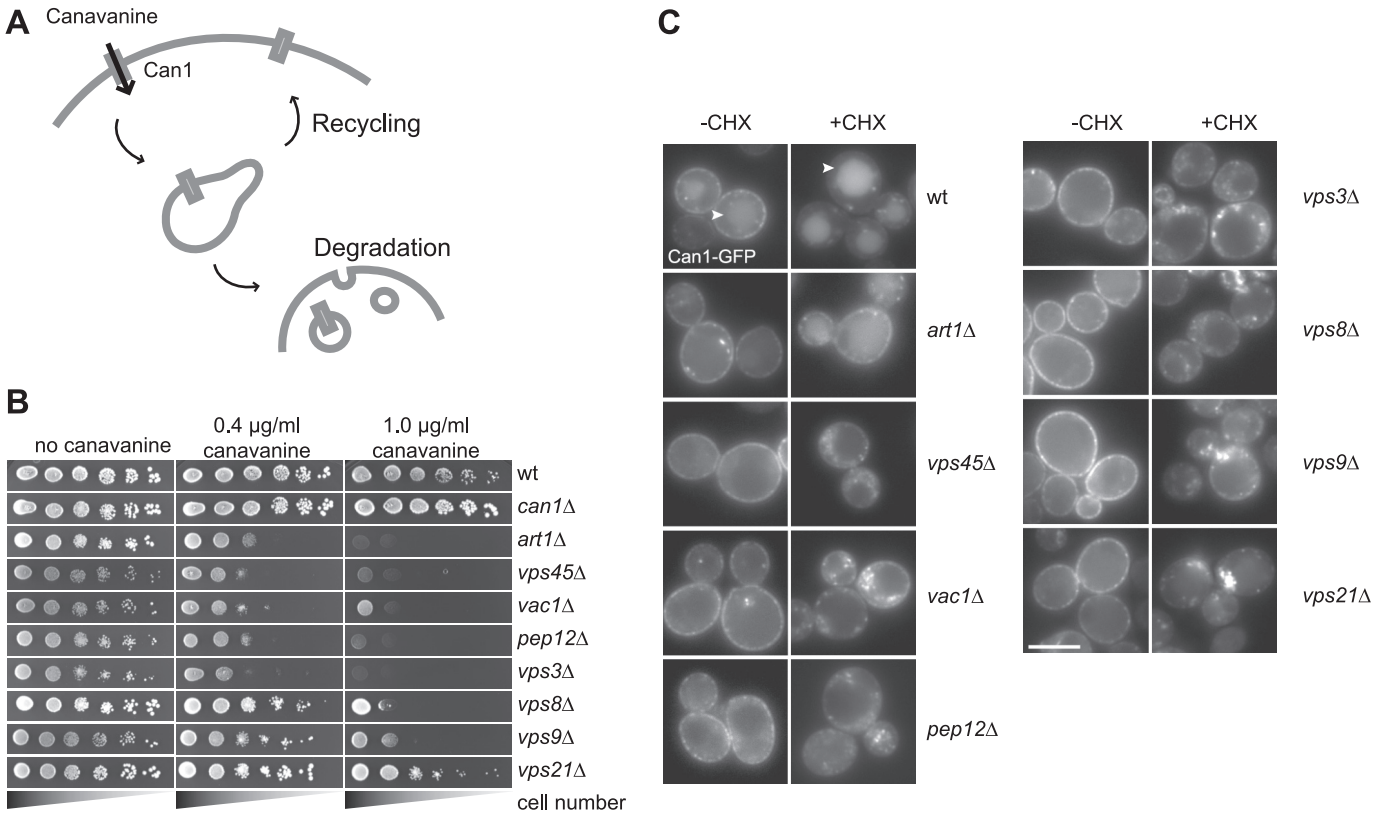

FIGURE 2. **Endocytic cargo sorting in class D mutants.** *A*, model of sorting of the Can1 permease from the plasma membrane via the recycling or degradation pathways. *B*, growth sensitivity to canavanine of class D mutants. The indicated strains were grown to logarithmic phase. Serial dilutions were spotted onto SDC plates without arginine containing the indicated canavanine concentrations. *C*, Can1 localization in class D mutants. Cells were grown to logarithmic phase in SDC-Arg. Endocytosis of Can1 was induced by cycloheximide (*CHX*) (50 μg/ml) treatment for 3 h and monitored by fluorescence microscopy. The vacuole lumen signal is indicated by *white arrowheads*. *Scale bar* = 5 μm.

therefore, explored the sorting of the arginine permease Can1 (36, 37). Can1 also transports the toxic arginine analog canavanine into cells. Sensitivity to this drug has been explored to identify mutants with altered amounts of Can1 on the cell surface because of defects in Can1 endocytosis or recycling (Fig. 2*A*). Growth sensitivity can be monitored with a simple plate assay (36, 37). In wild-type cells, Can1 is continuously sorted from the plasma membrane to the vacuole for degradation if cells experience an excess of substrate. Cells are thus resistant to a certain concentration of the toxic canavanine drug, similar to *can1*Δ cells (Fig. 2*B*). In endocytosis mutants such as *art1*Δ, Can1 is stabilized on the plasma membrane, which results in increased canavanine uptake and growth sensitivity. As shown in Fig. 2*B*, all class D deletion strains showed growth sensitivity to canavanine, consistent with a defect in the sorting of Can1 to the vacuole. Although most of the mutants had severe defects comparable with *art1*Δ, the *vps8*Δ, *vps21*Δ, and *vps9*Δ mutants showed a milder defect. The same mutants also displayed a weaker defect in Cps1 sorting (Fig. 1*C*).

To monitor the behavior of the Can1 permease in cells, we followed the localization of the GFP-tagged version. Under standard growth conditions, the permease is localized at the plasma membrane and in the vacuole lumen in wild-type cells (Fig. 2*C*, *left panel*). In *art1*Δ, the luminal vacuolar signal is absent because Can1 is not sorted into the endocytic pathway (37). All class D mutants showed a similar phenotype like *art1*Δ (Fig. 2*C*, *left panel*), which might indicate a defect in endocytosis (see below). The uptake and degradation of Can1 can be induced by addition of cycloheximide, which activates a signaling pathway via TORC1 (38, 39). Upon incubation with cycloheximide, Can1 is sorted to the vacuole lumen in wild-type cells, whereas it stained the plasma membrane in the *art1*Δ mutant (Fig. 2*C*, *right panel*). Surprisingly, all class D mutants showed accumulation of Can1 in intracellular puncta (Fig. 2*C*, *right panel*). This indicates that these cells are able to endocytose Can1 but are defective in Can1 sorting to the vacuole. Recycling from these intracellular structures to the plasma membrane is probably still possible and might explain the canavanine sensitivity phenotype. Overall, we conclude that protein transport along the endocytic pathway is strongly impaired in a group of class D mutants (*vps45*Δ, *pep12*Δ, *vac1*Δ, and *vps3*Δ) but only partially in *vps8*Δ, *vps21*Δ, and *vps9*Δ mutants, which suggests some redundancy in the endolysosomal trafficking (see below).

Overlapping and Distinct Functions of Vac1 and CORVET—Two Sec1/Munc18 proteins, Vps33 (CORVET) and Vps45, operate along the endocytic pathway. It has been shown that an excess of Vps45 cannot restore the wild-type phenotype in the *vps33*Δ mutant, presumably because of its interaction with a distinct set of SNAREs (26). We therefore used the same overexpression strategy to ask whether the Vac1 tether would compensate for the endosomal sorting defects observed in

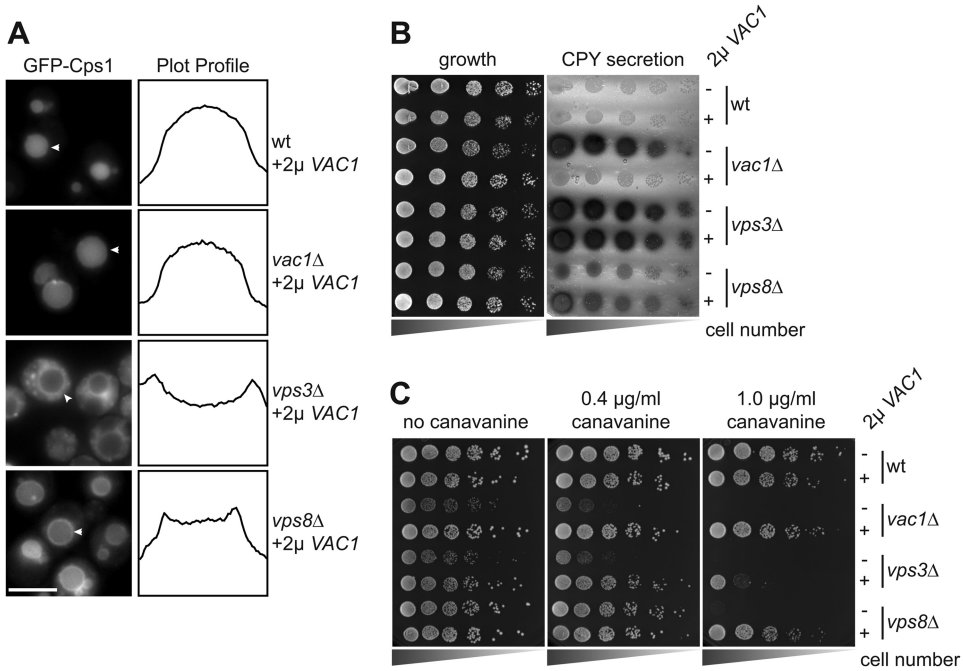

FIGURE 3. **Vac1 overproduction rescues endocytic but not biosynthetic sorting defects of CORVET mutants.** *A*, analysis of GFP-Cps1 sorting to the vacuole lumen. Strains carrying deletions of the *VAC1*, *VPS3*, or *VPS8* genes and expressing GFP-tagged Cps1 were transformed with a 2-μ plasmid coding for Vac1 before analysis by fluorescence microscopy. Fluorescence intensity profiles of representative vacuoles (*white arrowheads*) are shown. *Scale bar* = 5 μm. *B*, CPY sorting in CORVET mutants. Strains with and without additional Vac1 were grown on synthetic medium containing 2% fructose. Invertase activity was measured by overlaying the plates with developer solution (see "Experimental Procedures"). *C*, growth sensitivity of CORVET mutants to canavanine is rescued by Vac1 overproduction. Wild-type and mutant strains carrying the 2-μ plasmid coding for Vac1 were spotted on plates with canavanine as in Fig. 2*B*.

CORVET mutants. For this, we overexpressed Vac1 and initially monitored Cps1 sorting, which remained defective in both CORVET mutants (Fig. 3*A*; see Fig. 1*B* for comparison). To obtain a more quantitative readout of sorting events in the biosynthetic pathway, we analyzed the secretion of CPY using a plate assay where the release of a CPY invertase fusion protein from cells is monitored. Neither the *vps3*Δ nor the milder *vps8*Δ mutant were rescued by Vac1 overexpression (Fig. 3*B*). However, when we analyzed endocytic sorting by looking at Can1, Vac1 was able to rescue the defect of the *vps8*Δ and, partially, of the *vps3*Δ mutant (Fig. 3*C*). This indicates that Vac1 and CORVET have some overlap in endocytic transport but not in the sorting of biosynthetic cargo to the vacuole.

CORVET Deletions Differ in Their Ultrastructural Phenotypes from the vac1 Mutant—As another readout for differences between CORVET mutants and other class D fusion factors, we turned to ultrastructural analyses. Previous studies of class D mutants revealed an accumulation of 40- to 50-nm vesicles or vesicle clusters proximal to the vacuole, in agreement with their role as fusion factors (33, 40–44). We repeated this analysis to perform an accurate side-by-side comparison between all class D mutants, including the *vps3*Δ strain that has not been analyzed morphologically previously. As shown in Fig. 4, we could reveal clear ultrastructural differences between the class D mutants and classify them into three distinct groups. The first group only comprises the *vps45* knockout. In agreement with a previous study (33), these cells have the most severe phenotype of all class D mutants, with a multitude of vesicles dispersed throughout the cytoplasm when compared with the wild type (Fig. 4, *A* and *B*; quantified in *I*). This phenotype is consistent with the ability of Vps45 to associate with more than one SNARE to support fusion at both the early and late endosomes (45–47).

The second set of mutants includes *vac1*Δ and *pep12*Δ, characterized by multiple cytoplasmic vesicles that were, however, less abundant than in *vps45*Δ cells (Fig. 4, *C*, *D*, and *I*). These strains also accumulated large, partially stacked structures with dense content (*arrows*), which we interpret as endosomal intermediates (quantified in Fig. 4*I*). The remaining four mutants, *vps9*Δ, *vps21*Δ, *vps3*Δ, and *vps8*Δ, contained few vesicles compared with any of the other mutants, although clearly more than wild-type cells (Fig. 4, *E*–*H* and *I*). In addition, more dense endosomal structures devoid of luminal vesicles were observed (Fig. 4, *F*′–*H*′), which sometimes were also stacked (*F*′, *G*′, and *H*′). The double deletion strains *vps45*Δ *vps3*Δ and *vps45*Δ *vps8*Δ exhibited a phenotype identical to that of the *vps45*Δ cells (not shown), indicating that Vps45 probably acts upstream of CORVET in the endosomal sorting pathway, in agreement with earlier proposals (48). However, we did not observe the vesicle clusters reported before in *vps45*Δ mutants (33), presumably because of the different strain background. In summary, we conclude that the CORVET mutants have a very similar phenotype to v*ps21*Δ and *vps9*Δ but are distinct from the *vac1*Δ phenotype, indicating that CORVET acts separately along the endosomal system.

CORVET Localizes to Endosomes Independently of Vac1—To further address whether CORVET and Vac1 would act independently of each other, we analyzed their localization to endosomes. In a first set of experiments, we monitored the localization of GFP/dsRed-tagged Vps45, Pep12, and Vac1 in CORVET deletion mutants and observed largely dispersed signals with some remaining dot-like structures (Fig. 5*A*). A similar diffuse

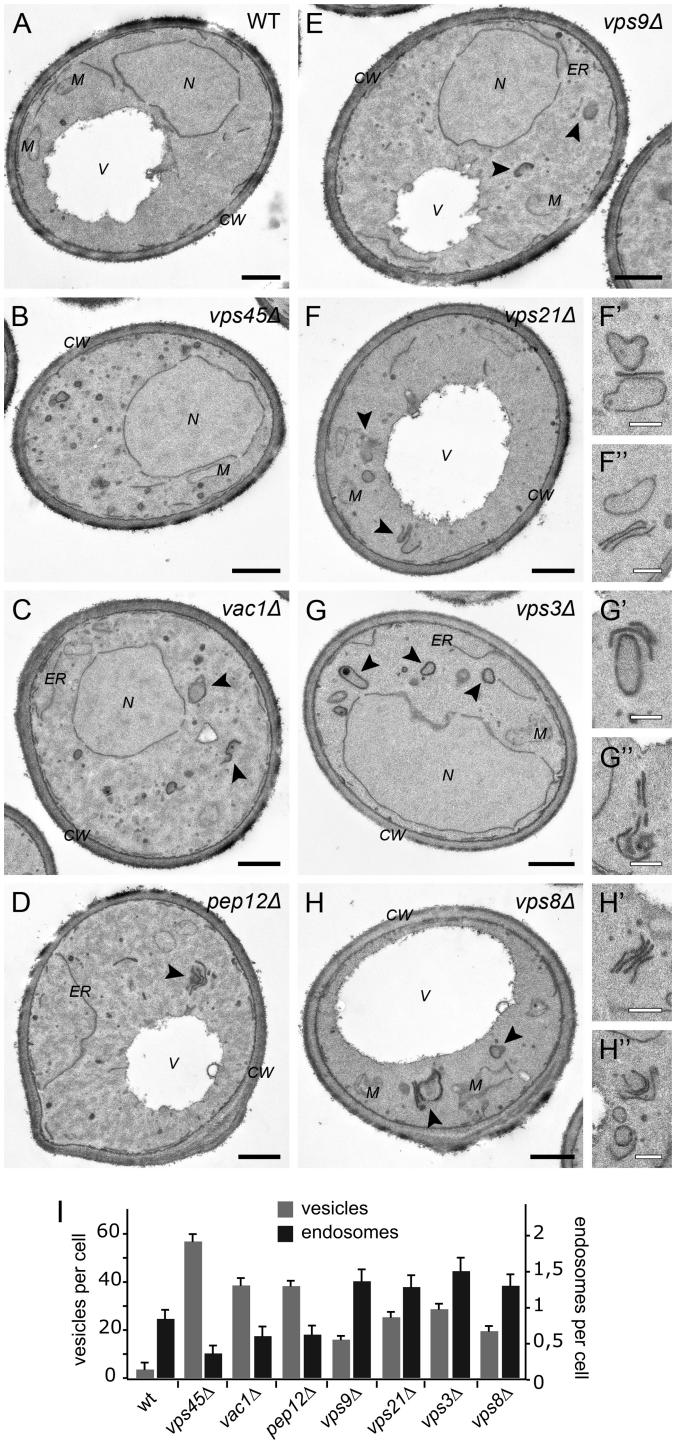

FIGURE 4. **Ultrastructural analysis of class D mutants.** Strains with the indicated deletions (*A-H*) were grown in logarithmic phase, embedded in Spurr's resin, and processed for electron microscopy. Putative endosomal structures are indicated by *black arrows*, and enlarged views are illustrated to the *right*. *Black scale bars* = 500 nm; *white scale bars* = 200 nm. *N*, nucleus; *M*, mitochondria; *ER*, endoplasmic reticulum; *V*, vacuole; *CW*, cell wall. *I*, quantification of vesicles and endosomal structures per cell. For each cell type structure, 50 individual cells were counted (data are mean ± S.E.). See "Experimental Procedures" for details.

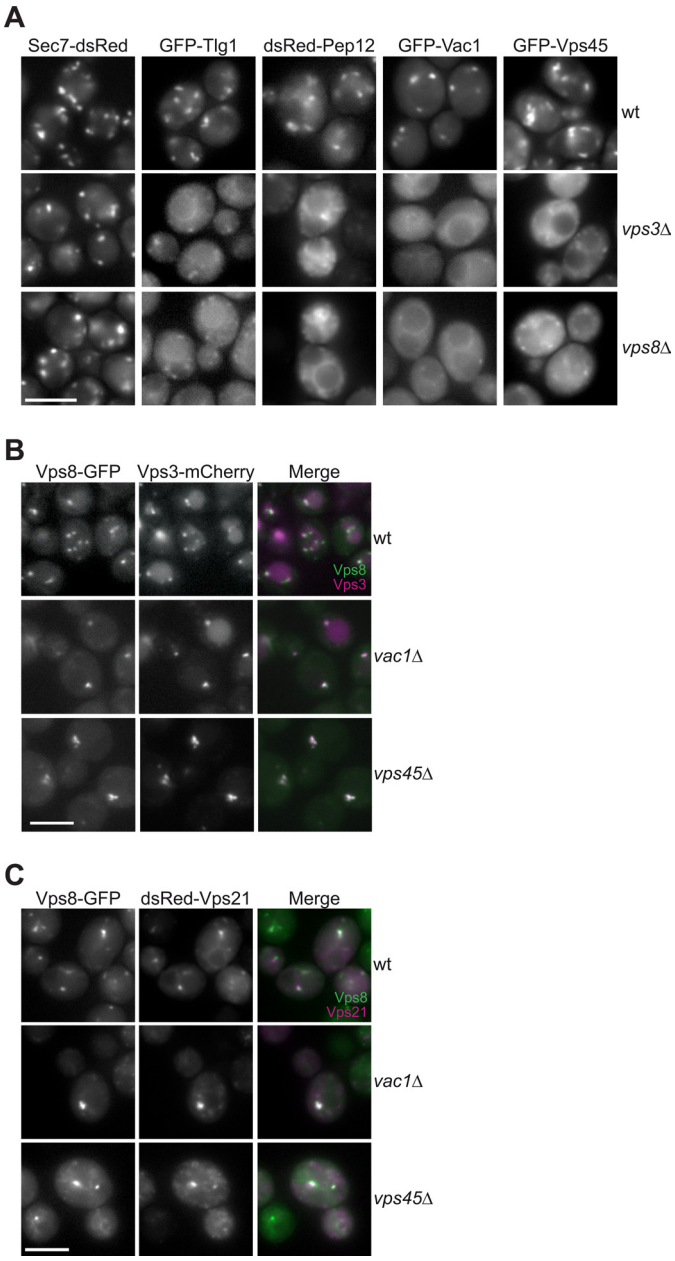

FIGURE 5. **CORVET localizes independently of Vac1 and Vps45 to endosomes.** *A*, effect of CORVET deletion on the localization of endosomal marker proteins. Fluorescently tagged Sec7, Tlg1, Pep12, Vac1, and Vps45 were analyzed by microscopy. *B*, colocalization of Vps3 and Vps8 in class D mutants. Vps3 was tagged with 3xmCherry in the Vps8-GFP background strain and expressed in WT and the vac1Δ and *vps45*Δ mutants. Both fluorophores were visualized by fluorescence microscopy. *C*, CORVET-positive structures correspond to endosomes. Colocalization of dsRed-tagged Vps21 and Vps8-GFP was performed as in *B*. *Scale bars* = 5 μm.

signal was observed for the early endosomal SNARE Tlg1. As the SNAREs Pep12 and Tlg1 are membrane-bound, the diffuse fluorescent signal in CORVET mutants likely corresponds to the small vesicular structures observed in our EM analyses (Fig. 4, *G* and *H*). CORVET deletions did, however, not affect the localization of Sec7 to the Golgi, and both mutants still displayed endosomes, which are labeled by endocytosed Can1 (Fig. 2*C*).

We then asked, in reverse, whether CORVET subunits would still localize if Vac1 or Vps45 were deleted. To be able to monitor CORVET behavior simultaneously, we tagged Vps3 and Vps8 with different fluorophores. Both proteins colocalized to the same dots in wild-type and *vac1*Δ and *vps45*Δ mutants, even though the dots appeared to be more prominent in both

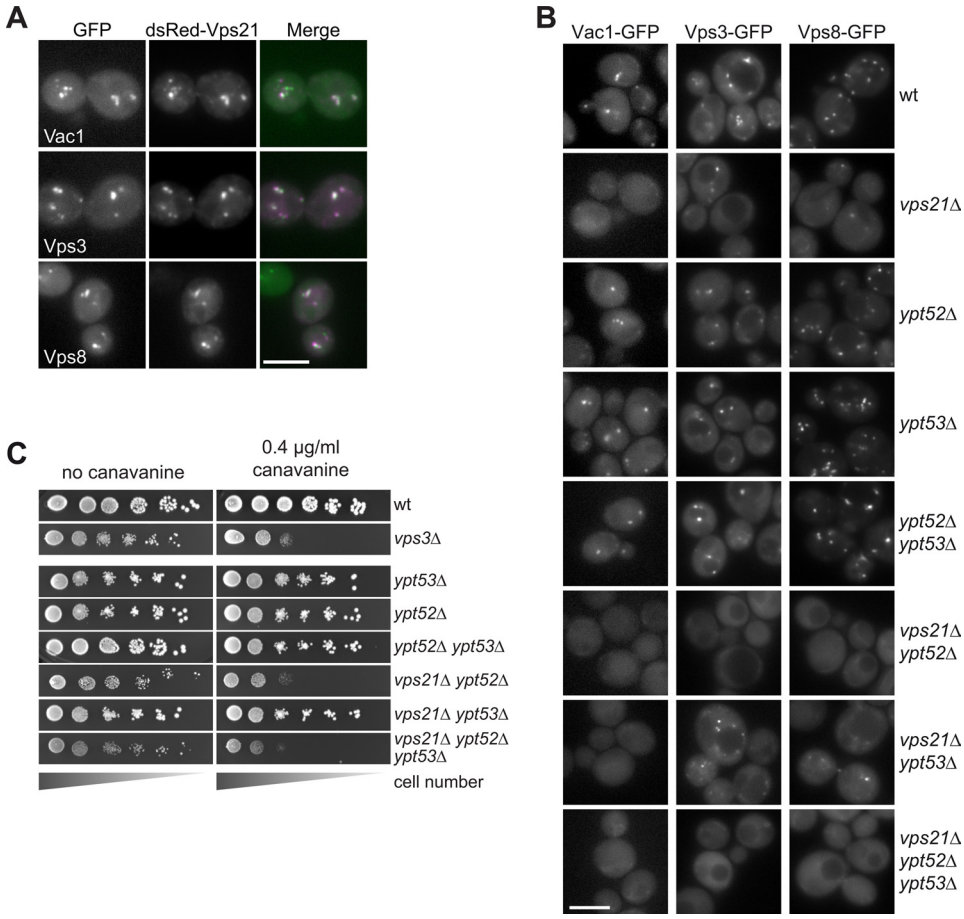

FIGURE 6. **Localization and function of CORVET requires Rab5 homologs.** *A*, colocalization of Vps21 with Vps3, Vps8, and Vac1. Microscopy of dsRed-tagged Vps21 expressed from centromeric (CEN) plasmids in the Vps3-GFP, Vps8-GFP, and Vac1-GFP background strains. *Scale bar* = 5 μm. *B*, CORVET localization depends on Vps21 and Ypt52, whereas Vac1 localization is Vps21-specific. GFP-tagged Vac1, Vps3, and Vps8 were localized in the indicated single, double, and triple deletion strains. *Scale bar* = 5 μm. *C*, growth sensitivity of Rab5 deletions on canavanine-containing plates. Growth of WT and *vps3*Δ deletion strains are shown in comparison to the Rab5 homolog deletion strains. The assay was performed as in Fig. 2*B*.

mutants (Fig. 5*B*). To confirm that these dots were indeed endosomes, we colocalized Vps8 with Vps21 and observed both in the same structures (Fig. 5*C*). This indicates that CORVET localizes to endosomes independently of the Vac1 tether or Vps45. Our data are therefore consistent with a separate role of CORVET at endosomes.

CORVET Can Use Two Rab5 Proteins to Get to Endosomes and Vac1 Only One—We next asked whether we could further dissect the differences between CORVET and Vac1 by comparing the cross-talk with the Rab GTPase Vps21. Both CORVET and Vac1 have been described as Vps21 effectors (12, 14, 16, 17, 23, 24). In agreement with this, all three GFP-tagged proteins colocalized with Vps21 (Fig. 6*A*). Next, we asked whether we could further distinguish the two tethers by following their localization to endosomes in Rab5 deletion mutants. It was shown before that loss of Vps21 can be compensated partially by the two other Rab5 homologs, Ypt52 and Ypt53 (50, 51). When we monitored the localization of all GFP-tagged tethers in the *vps21*Δ mutant, we observed no dot localization of Vac1 and a loss of Vps8 and Vps3 endosomal localization, even though some dots were still detectable (Fig. 6*B*). For CORVET, we asked whether any of the other two homologs might compensate and thus generate double mutants. Only upon deletion of Ypt52 in addition to Vps21, CORVET became entirely mislocalized, whereas a deletion of Ypt53 was without effect. This indicates that CORVET can use two Rab5 homologs to localize to endosomes, whereas Vac1 is specific for Vps21. It has been reported previously that Vac1 remains membrane-bound in *vps21*Δ cells (24), which may explain the different phenotypes of *vac1*Δ and *vps21*Δ mutants in our ultrastructure analysis (Fig. 4).

The observation of a compensatory Rab function for CORVET localization is supported by the canavanine assay. As mentioned before, the *vps21*Δ and *vps3*Δ mutants differed in their canavanine sensitivity, with *vps3*Δ as the more severe mutant (Fig. 2*B*). If Vps21 can function together with Vps3 but the *vps21*Δ mutant can be partially rescued by Ypt52, we would expect that the *vps21*Δ *ypt52*Δ double mutant would behave like *vps3*Δ cells. This was indeed observed (Fig. 6*C*). We thus conclude that CORVET can use both Vps21 and Ypt52 for localization and function.

Uncovering of a Second Rab5 GEF for CORVET Function—It was thought previously that Vps9 is the only GEF for Rab5 proteins in yeast. We were therefore puzzled that the *vps9*Δ mutant had a weak phenotype in the canavanine growth assay, like the *vps21*Δ mutant (Fig. 2*B*). Muk1 is another protein with a Vps9 homology domain that had been identified in the genome (29) but never characterized in yeast. We asked

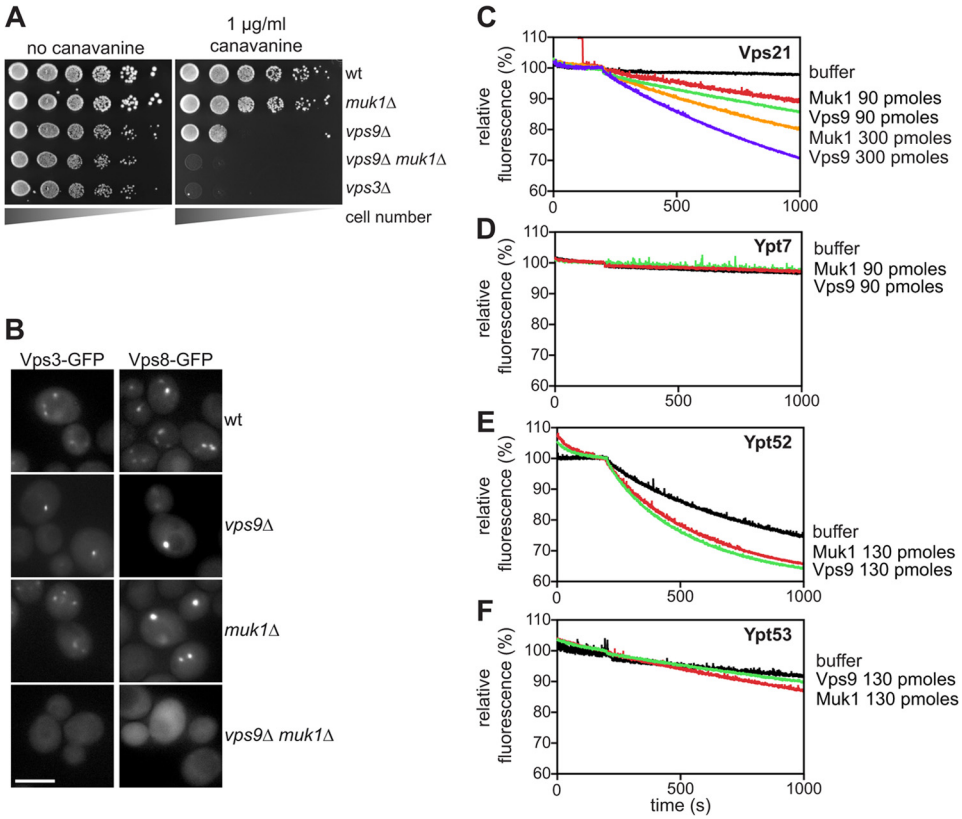

FIGURE 7. **Identification of overlapping Rab5 GEF activity in the endocytic pathway.** *A*, growth sensitivity on canavanine-containing plates. Single and double deletions of *vps9*Δ and *muk1*Δ were analyzed in comparison to wild-type and *vps3*Δ cells (see Fig. 2*C* for details). *B*, localization of Vps3 and Vps8 to endosomal dots is only abolished upon loss of both GEFs. Vps3-GFP and Vps8-GFP expressed from CEN plasmids were localized by fluorescence microscopy in the indicated single and double deletion strains. *Scale bar* = 5 μm. *C–F*, Muk1 triggers nucleotide exchange on Rab5 proteins but not Ypt7. 500 pmol of GST-Rabs preloaded with MANT-GDP was used in the assays. The indicated concentrations of MBP-Muk1 or MBP-Vps9 were added, and the reaction was equilibrated for 200 s before addition of 0.1 mM GTP. Excitation of MANT-fluorophore was performed at 366 nm, and emission was detected at 443 nm. Reactions are shown for each Rab-GEF combination for Vps21 (*C*), Ypt7 (*D*), Ypt52 (*E*), and Ypt53 (*F*).

whether Muk1 might compensate for the absence of Vps9 and thus monitored canavanine sensitivity in a *vps9*Δ *muk1*Δ double mutant. Indeed, we observed the same canavanine sensitivity as for *vps3*Δ or the *vps21*Δ *ypt52*Δ double mutant (Figs. 6*C* and 7*A*). We next asked whether the CORVET subunits would indeed require both Vps9 and Muk1 for localization to endosomes. In either deletion, we still observed dot-like structures for GFP-tagged Vps3 or Vps8. However, CORVET localization to endosomes was completely abolished in the *vps9*Δ *muk1*Δ double mutant (Fig. 7*B*). This suggests that Muk1 and Vps9 can both activate Rab5 homologs in yeast and thus compensate for the lack of each other. One homolog seems to be sufficient to localize the CORVET subunits within the endosomal system.

To confirm the role of Muk1 in Vps21 activation, we tested its activity in fluorescent GEF assays and observed that Muk1, like the previously characterized GEF Vps9, was able to stimulate nucleotide release on Vps21 (Fig. 7*C*) but not Ypt7 (*D*). Muk1 also showed GEF activity toward Ypt52 (Fig. 7*E*), which has higher intrinsic nucleotide release compared with Vps21 but only residual activity for Ypt53 (*F*). This indicates that the activation of yeast Rab5 homologs depends on two overlapping GEFs.

DISCUSSION

In this study, we set out to unravel the cross-talk and potential unique functions of CORVET and other endosomal fusion factors. We showed that CORVET requires activated Rab5 homologs Vps21 or Ypt52 to localize to endosomes, consistent with a redundant role of these two Rabs in yeast (50). Moreover, we uncovered that two GEFs, the likely GEF Muk1 and Vps9, which is equivalent to mammalian Rabex-5, can activate the Rab5 proteins. This is consistent with the morphological differences between the different class D mutants (*vps3*Δ, *vps8*Δ, *vps21*Δ, and *vps9*Δ) showing the same overall phenotype of less vesicles and more apparent endosomes. Moreover, the other tether Vac1 could not compensate for CORVET absence in the transport and sorting of hydrolases to the vacuole, although we observed suppression of the Can1 sensitivity phenotype. As endosomal localization of CORVET can occur in the absence of Vac1, we consider it likely that CORVET can act independently in fusion.

CORVET has been considered a tethering factor largely on the basis of its homology to HOPS (12, 52). However, to date no functional assay for CORVET function has been presented. In addition, it had remained unclear if endosomal tethering factors cooperated in fusion. Our data presented here make it more likely that CORVET operates independently of Vac1 in the tethering of Golgi-derived vesicles with endosomes and endosome-endosome fusion, which is likely a prerequisite of efficient sorting into multivesicular bodies. In contrast, other class D proteins, like Vps45 and Vac1, might have a major role

in the consumption of endocytic vesicles at endosomes, as revealed by the accumulation of vesicles in the corresponding deletion mutants (23, 24, 33, 48). It is therefore not unexpected that Vac1 can only partially suppress the endocytic transport defect in CORVET mutants.

It has been shown recently that hyperactive Rab5 homolog Vps21 can trigger the formation of stacked endosomal compartments that mimic the absence of ESCRT proteins (53). On the basis of our data, we consider it likely that CORVET drives the stacking of endosomes, although it should be kept in mind that only the Vps8 subunit localizes to the class E compartment and is sufficient to cluster multivesicular bodies (14). Interestingly, Russell *et al.* 53 did not observe an multivesicular body sorting defect in the *vps21*Δ mutant, even though we (this study) and others (50) did observe this. We consider it likely that these divergent observations are due to the weaker phenotype of the mutant. In agreement with this, CORVET localization is also maintained partially in *vps21*Δ mutant and is only lost if another Rab5 homolog, Ypt52, is deleted.

Even though the two CORVET-specific subunits Vps3 and Vps8 colocalize efficiently and behave similarly in the absence of Rab5 proteins, the phenotype of each deletion differs. *vps8*Δ cells are less sensitive to the drug canavanine and have a weak CPY secretion phenotype and Cps1 sorting defect (Ref. 26 and this study). We showed before that in the *vps8*Δ mutant, the HOPS subunit Vps41 fills the gap within the CORVET complex, resulting in a Vps3-Vps41-class C hybrid complex (12). In contrast, *vps3*Δ cells contain an incomplete pentamer comprising Vps8 and the four class C proteins that are shared by HOPS and CORVET (17). This suggests that only three complexes (CORVET, HOPS, and the Vps3-Vps41-class C hybrid) are active as tethering or transition complexes. Although the hybrid complex is a very minor species in wild-type cells (12), it may act in fusion (17) or stabilize an eventual transition between CORVET and HOPS.

In agreement with their postulated function as a tethering complex, both Vps3 and Vps8 interact genetically and physically with the Rab GTPase Vps21 (12, 14, 16, 26). Our recent analysis of the HOPS complex (18) would place Vps3 and Vps8 at opposite ends of an elongated hexamer, and CORVET could tether Vps21-positive membranes prior to their SNARE-dependent fusion. Here we further demonstrate that Ypt52 can also mediate the endosomal localization of CORVET. It remains to be determined whether Ypt52 is just a backup Rab for Vps21 or functions in specific fusion events. Neither our study nor the recent in-depth analysis of Merz and colleagues (50) on Rab5 homologs was able to reveal a Ypt52-specific function. Similarly, mammals contain three isoforms of Rab5 (a, b, and c) with overlapping and specific functions along the endocytic pathway (55). In addition, the other two members of the Rab5 subfamily, Rab21 and Rab22, have been involved in endosomal trafficking (49, 54, 56)

We show that Muk1, a protein with a Vps9 domain (29), is able to compensate for the loss of Vps9 and displays GEF activity toward Rab5 proteins. Despite these findings we cannot yet explain the need of a second Rab5 GEF in yeast. It would be possible that Muk1-specific domains provide additional levels of Rab5 modulation. In mammals, the functional redundancy is even higher, and at least eight Vps9 domain-containing proteins (Rabex-5, RIN1, RIN2, RIN3, GAPVD1, ALSIN, ALS2CL, and ANKRD27) show GEF activity for the Rab5 subfamily (29).

The Rab5-dependent localization of CORVET agrees nicely with our previous observations that the homologous HOPS complex requires the yeast Rab7 homolog Ypt7 for its vacuole localization (18). We thus conclude that both tethering complexes depend on their active Rab to bind to the appropriate organelle membrane.

Future studies will be necessary to reconstitute *in vitro* the tethering activity of the CORVET complex and dissect the interface between CORVET and HOPS function. Additionally, the interaction of the CORVET complex with the endosomal SNAREs remains to be established. Our findings now assign the different fusion complexes to separate reactions along the organelles of the endolysosomal system, which should facilitate further analysis.

REFERENCES

1. Rink, J., Ghigo, E., Kalaidzidis, Y., and Zerial, M. (2005) Rab conversion as a mechanism of progression from early to late endosomes. *Cell* **122,** 735–749
2. Bowers, K., and Stevens, T. (2005) Protein transport from the late Golgi to the vacuole in the yeast *Saccharomyces cerevisiae*. *Biochim. Biophys. Acta* **1744,** 438–454
3. Poteryaev, D., Datta, S., Ackema, K., Zerial, M., and Spang, A. (2010) Identification of the switch in early-to-late endosome transition. *Cell* **141,** 497–508
4. Epp, N., Rethmeier, R., Krämer, L., and Ungermann, C. (2011) Membrane dynamics and fusion at late endosomes and vacuoles. Rab regulation, multisubunit tethering complexes and SNAREs. *Eur J. Cell Biol.* **90,** 779–785
5. Bröcker, C., Engelbrecht-Vandré, S., and Ungermann, C. (2010) Multisubunit tethering complexes and their role in membrane fusion. *Curr. Biol.* **20,** R943–52
6. Cullen, P. J. (2008) Endosomal sorting and signalling. An emerging role for sorting nexins. *Nat. Rev. Mol. Cell Biol.* **9,** 574–582
7. Yu, I.-M., and Hughson, F. M. (2010) Tethering factors as organizers of intracellular vesicular traffic. *Annu. Rev. Cell Dev. Biol.* **26,** 137–156
8. Seals, D. F., Eitzen, G., Margolis, N., Wickner, W. T., and Price, A. (2000) A Ypt/Rab effector complex containing the Sec1 homolog Vps33p is required for homotypic vacuole fusion. *Proc. Natl. Acad. Sci. U.S.A.* **97,** 9402–9407
9. Spang, A. (2009) On the fate of early endosomes. *Biol. Chem.* **390,** 753–759
10. Wurmser, A. E., Sato, T. K., and Emr, S. D. (2000) New component of the vacuolar class C-Vps complex couples nucleotide exchange on the Ypt7 GTPase to SNARE-dependent docking and fusion. *J. Cell Biol.* **151,** 551–562
11. Bonifacino, J. S., and Hurley, J. H. (2008) Retromer. *Curr. Opin. Cell Biol.* **20,** 427–436
12. Peplowska, K., Markgraf, D. F., Ostrowicz, C. W., Bange, G., and Ungermann, C. (2007) The CORVET tethering complex interacts with the yeast Rab5 homolog Vps21 and is involved in endo-lysosomal biogenesis. *Dev. Cell* **12,** 739–750
13. Teis, D., Saksena, S., and Emr, S. D. (2009) SnapShot. The ESCRT machinery. *Cell* **137,** 182–182.e1
14. Markgraf, D. F., Ahnert, F., Arlt, H., Mari, M., Peplowska, K., Epp, N., Griffith, J., Reggiori, F., and Ungermann, C. (2009) The CORVET subunit Vps8 cooperates with the Rab5 homolog Vps21 to induce clustering of late endosomal compartments. *Mol. Biol. Cell* **20,** 5276–5289
15. Pawelec, A., Arsi, J., and Kölling, R. (2010) Mapping of Vps21 and HOPS binding sites in Vps8 and effect of binding site mutants on endocytic trafficking. *Eukaryotic. Cell* **9,** 602–610
16. Plemel, R. L., Lobingier, B. T., Brett, C. L., Angers, C. G., Nickerson, D. P., Paulsel, A., Sprague, D., and Merz, A. J. (2011) Subunit organization and Rab interactions of Vps-C protein complexes that control endolysosomal membrane traffic. *Mol. Biol. Cell* **22,** 1353–1363

17. Ostrowicz, C. W., Bröcker, C., Ahnert, F., Nordmann, M., Lachmann, J., Peplowska, K., Perz, A., Auffarth, K., Engelbrecht-Vandré, S., and Ungermann, C. (2010) Defined subunit arrangement and Rab interactions are required for functionality of the HOPS tethering complex. *Traffic* **11,** 1334–1346
18. Bröcker, C., Kuhlee, A., Gatsogiannis, C., Balderhaar, H. J., Hönscher, C., Engelbrecht-Vandré, S., Ungermann, C., and Raunser, S. (2012) Molecular architecture of the multisubunit homotypic fusion and vacuole protein sorting (HOPS) tethering complex. *Proc. Natl. Acad. Sci. U.S.A.* **109,** 1991–1996
19. Subramanian, S., Woolford, C. A., and Jones, E. W. (2004) The Sec1/Munc18 protein, Vps33p, functions at the endosome and the vacuole of *Saccharomyces cerevisiae*. *Mol. Biol. Cell* **15,** 2593–2605
20. Pieren, M., Schmidt, A., and Mayer, A. (2010) The SM protein Vps33 and the t-SNARE H(abc) domain promote fusion pore opening. *Nat. Struct. Mol. Biol.* **17,** 710–717
21. Krämer, L., and Ungermann, C. (2011) HOPS drives vacuole fusion by binding the vacuolar SNARE complex and the Vam7 PX domain via two distinct sites. *Mol. Biol. Cell* **22,** 2601–2611
22. Hama, H., Tall, G. G., and Horazdovsky, B. (1999) Vps9p is a guanine nucleotide exchange factor involved in vesicle-mediated vacuolar protein transport. *J. Biol. Chem.* **274,** 15284–15291
23. Peterson, M. R., Burd, C. G., and Emr, S. D. (1999) Vac1p coordinates Rab and phosphatidylinositol 3-kinase signaling in Vps45p-dependent vesicle docking/fusion at the endosome. *Curr. Biol.* **9,** 159–162
24. Tall, G. G., Hama, H., DeWald, D. B., and Horazdovsky, B. F. (1999) The phosphatidylinositol 3-phosphate binding protein Vac1p interacts with a Rab GTPase and a Sec1p homologue to facilitate vesicle-mediated vacuolar protein sorting. *Mol. Biol. Cell* **10,** 1873–1889
25. Raymond, C. K., O'Hara, P. J., Eichinger, G., Rothman, J. H., and Stevens, T. H. (1990) Molecular analysis of the yeast VPS3 gene and the role of its product in vacuolar protein sorting and vacuolar segregation during the cell cycle. *J. Cell Biol.* **111,** 877–892
26. Horazdovsky, B. F., Cowles, C. R., Mustol, P., Holmes, M., and Emr, S. D. (1996) A novel RING finger protein, Vps8p, functionally interacts with the small GTPase, Vps21p, to facilitate soluble vacuolar protein localization. *J. Biol. Chem.* **271,** 33607–33615
27. Raymond, C. K., Howald-Stevenson, I., Vater, C. A., and Stevens, T. H. (1992) Morphological classification of the yeast vacuolar protein sorting mutants. Evidence for a prevacuolar compartment in class E vps mutants. *Mol. Biol. Cell* **3,** 1389–1402
28. Weisman, L. S., Emr, S. D., and Wickner, W. T. (1990) Mutants of *Saccharomyces cerevisiae* that block intervacuole vesicular traffic and vacuole division and segregation. *Proc. Natl. Acad. Sci. U.S.A.* **87,** 1076–1080
29. Carney, D. S., Davies, B. A., and Horazdovsky, B. F. (2006) Vps9 domain-containing proteins. Activators of Rab5 GTPases from yeast to neurons. *Trends Cell Biol.* **16,** 27–35
30. Janke, C., Magiera, M. M., Rathfelder, N., Taxis, C., Reber, S., Maekawa, H., Moreno-Borchart, A., Doenges, G., Schwob, E., Schiebel, E., and Knop, M. (2004) A versatile toolbox for PCR-based tagging of yeast genes. New fluorescent proteins, more markers and promoter substitution cassettes. *Yeast* **21,** 947–962
31. Cabrera, M., Ostrowicz, C. W., Mari, M., LaGrassa, T. J., Reggiori, F., and Ungermann, C. (2009) Vps41 phosphorylation and the Rab Ypt7 control the targeting of the HOPS complex to endosome-vacuole fusion sites. *Mol. Biol. Cell* **20,** 1937–1948
32. Cabrera, M., Langemeyer, L., Mari, M., Rethmeier, R., Orban, I., Perz, A., Bröcker, C., Griffith, J., Klose, D., Steinhoff, H.-J., Reggiori, F., Engelbrecht-Vandré, S., and Ungermann, C. (2010) Comment on phosphorylation of a membrane curvature-sensing motif switches function of the HOPS subunit Vps41 in membrane tethering. *J. Cell Biol.* **191,** 845–859
33. Cowles, C. R., Emr, S. D., and Horazdovsky, B. F. (1994) Mutations in the VPS45 gene, a SEC1 homologue, result in vacuolar protein sorting defects and accumulation of membrane vesicles. *J. Cell Sci.* **107,** 3449–3459
34. Nordmann, M., Cabrera, M., Perz, A., Bröcker, C., Ostrowicz, C., Engelbrecht-Vandré, S., and Ungermann, C. (2010) The Mon1-Ccz1 complex is the GEF of the late endosomal Rab7 homolog Ypt7. *Curr. Biol.* **20,** 1654–1659
35. Odorizzi, G., Babst, M., and Emr, S. (1998) Fab1p PtdIns(3)P 5-kinase function essential for protein sorting in the multivesicular body. *Cell* **95,** 847–858
36. Shi, Y., Stefan, C. J., Rue, S. M., Teis, D., and Emr, S. D. (2011) Two novel WD40 domain-containing proteins, Ere1 and Ere2, function in the retromer-mediated endosomal recycling pathway. *Mol. Biol. Cell* **22,** 4093–4107
37. Lin, C. H., MacGurn, J. A., Chu, T., Stefan, C. J., and Emr, S. D. (2008) Arrestin-related ubiquitin-ligase adaptors regulate endocytosis and protein turnover at the cell surface. *Cell* **135,** 714–725
38. Binda, M., Péli-Gulli, M.-P., Bonfils, G., Panchaud, N., Urban, J., Sturgill, T. W., Loewith, R., and De Virgilio, C. (2009) The Vam6 GEF controls TORC1 by activating the EGO complex. *Mol. Cell* **35,** 563–573
39. MacGurn, J. A., Hsu, P.-C., Smolka, M. B., and Emr, S. D. (2011) TORC1 regulates Endocytosis via Npr1-mediated phosphoinhibition of a ubiquitin ligase adaptor. *Cell* **147,** 1104–1117
40. Webb, G. C., Hoedt, M., Poole, L. J., and Jones, E. W. (1997) Genetic interactions between a pep7 mutation and the PEP12 and VPS45 genes. Evidence for a novel SNARE component in transport between the *Saccharomyces cerevisiae* Golgi complex and endosome. *Genetics* **147,** 467–478
41. Horazdovsky, B. F., Busch, G. R., and Emr, S. D. (1994) VPS21 encodes a rab5-like GTP binding protein that is required for the sorting of yeast vacuolar proteins. *EMBO J.* **13,** 1297–1309
42. Woolford, C. A., Bounoutas, G. S., Frew, S. E., and Jones, E. W. (1998) Genetic interaction with vps8–200 allows partial suppression of the vestigial vacuole phenotype caused by a pep5 mutation in *Saccharomyces cerevisiae*. *Genetics* **148,** 71–83
43. Becherer, K. A., Rieder, S. E., Emr, S. D., and Jones, E. W. (1996) Novel syntaxin homologue, Pep12p, required for the sorting of lumenal hydrolases to the lysosome-like vacuole in yeast. *Mol. Biol. Cell* **7,** 579–594
44. Burd, C. G., Mustol, P. A., Schu, P. V., and Emr, S. D. (1996) A yeast protein related to a mammalian Ras-binding protein, Vps9p, is required for localization of vacuolar proteins. *Mol. Cell Biol.* **16,** 2369–2377
45. Bryant, N. J., and James, D. E. (2001) Vps45p stabilizes the syntaxin homologue Tlg2p and positively regulates SNARE complex formation. *EMBO J.* **20,** 3380–3388
46. Carpp, L. N., Ciufo, L. F., Shanks, S. G., Boyd, A., and Bryant, N. J. (2006) The Sec1p/Munc18 protein Vps45p binds its cognate SNARE proteins via two distinct modes. *J. Cell Biol.* **173,** 927–936
47. Furgason, M. L., MacDonald, C., Shanks, S. G., Ryder, S. P., Bryant, N. J., and Munson, M. (2009) The N-terminal peptide of the syntaxin Tlg2p modulates binding of its closed conformation to Vps45p. *Proc. Natl. Acad. Sci. U.S.A.* **106,** 14303–14308
48. Peterson, M. R., and Emr, S. D. (2001) The class C Vps complex functions at multiple stages of the vacuolar transport pathway. *Traffic* **2,** 476–486
49. Simpson, J. C., Griffiths, G., Wessling-Resnick, M., Fransen, J. A., Bennett, H., and Jones, A. T. (2004) A role for the small GTPase Rab21 in the early endocytic pathway. *J. Cell Sci.* **117,** 6297–6311
50. Nickerson, D. P., Russell, M. R., Lo, S.-Y., Chapin, H. C., Milnes, J. M., and Merz, A. J. (2012) Termination of isoform-selective Vps21/Rab5 signaling at endolysosomal organelles by Msb3/Gyp3. *Traffic* **13,** 1411–1428
51. Singer-Krüger, B., Stenmark, H., Düsterhöft, A., Philippsen, P., Yoo, J. S., Gallwitz, D., and Zerial, M. (1994) Role of three rab5-like GTPases, Ypt51p, Ypt52p, and Ypt53p, in the endocytic and vacuolar protein sorting pathways of yeast. *J. Cell Biol.* **125,** 283–298
52. Nickerson, D. P., Brett, C. L., and Merz, A. J. (2009) Vps-C complexes. Gatekeepers of endolysosomal traffic. *Curr. Opin. Cell Biol.* **21,** 543–551
53. Russell, M. R. G., Shideler, T., Nickerson, D. P., West, M., and Odorizzi, G. (2012) Class E compartments form in response to ESCRT dysfunction in yeast due to hyperactivity of the Vps21 Rab GTPase. *J. Cell Sci.* **125,** 5208–5220
54. Kauppi, M., Simonsen, A., Bremnes, B., Vieira, A., Callaghan, J., Stenmark, H., and Olkkonen, V. (2002) The small GTPase Rab22 interacts with EEA1 and controls endosomal membrane trafficking. *J. Cell Sci.* **115,** 899–911
55. Bucci, C., Lütcke, A., Steele-Mortimer, O., Olkkonen, V. M., Dupree, P., Chiariello, M., Bruni, C. B., Simons, K., and Zerial, M. (1995) Co-operative regulation of endocytosis by three Rab5 isoforms. *FEBS Lett.* **366,** 65–71
56. Pereira-Leal, J. B., and Seabra, M. C. (2001) Evolution of the Rab family of small GTP-binding proteins. *J. Mol. Biol.* **313,** 889–901